



## INVESTIGATION OF GEOTHERMAL ENERGY RESOURCE POTENTIAL USING AERO-MAGNETIC AND AERO-RADIOMETRIC DATA OF KANO, NIGERIA

\*<sup>1</sup>Yakubu, M. B., <sup>1</sup>Lawal, K. M., <sup>2</sup>Dewu, B. B. M., <sup>3</sup>Ikpokonte, A. E.

<sup>1</sup> Department of Physics, Ahmadu Bello University, Zaria

<sup>2</sup>Centre for Energy Research and Training, Ahmadu Bello University, Zaria

<sup>3</sup>Department of Geology, Ahmadu Bello University, Zaria

\*Corresponding authors' email: [bashaish12@gmail.com](mailto:bashaish12@gmail.com)

### ABSTRACT

This study focused on investigating the geothermal resource potential in Kano using high resolution aeromagnetic and radiometric data. A total of sixteen (16) sheets of aeromagnetic data with a block dimension of 55 km x 55 km were processed. Thus, the spectral centroid method which result from low wave number part of the wave number-scaled (depth to the centroid) and high-wave-number portion of the power spectrum (depth to the top) were estimated. Thus, the Curie point depth (CPD), geothermal gradient and heat flow were determined using appropriate parameters. The results showed that the CPD values range from 4.27 km to 19.59 km with an average of 11.83 km, and geothermal gradient ranges from 29.6 °C/km to 135.7 °C/m with an average of 82.7 °C/km while the heat flow ranges from 74 mW/m<sup>2</sup> to 339.2 mW/m<sup>2</sup> with the average of 206.6 mW/m<sup>2</sup>. Areas with high heat flow and shallow CPD could be prospective areas for geothermal energy. The values of the radiogenic heat obtained in the study area range from 0.15 to 2.77 μW/m<sup>3</sup>. It was observed that the highest radiogenic heat generation in the area is greater than the average radiogenic heat values in the continental crust. The information obtained from temperature to depth model reveals that, the Curie temperature could be reached at the depths of 6 km within the regions.

**Keywords:** Curie point depth, heat flow, geothermal gradient, radiogenic heat generation, temperature to depth variation.

### INTRODUCTION

Aeromagnetic and airborne radiometric data could be used in a variety of ways, to minimize noise, enhance particular aspects of the data and/or integrate with other geophysical data (Megwara *et al.*, 2013). Recent works by Nwankwo and Shehu (2015), Ezekiel (2019), Nwankwo and Sunday (2017), among others have shown great potential for geothermal heat flow in the Sokoto and Bida Basins respectively. Thus, geothermal resource (energy) can be extracted within the Earth and could be used either directly for heating applications or transform into electricity. The locations at which these resources are stored can be identified by estimating the Curie point depth from magnetic data over an area of interest. The Curie-point depth (CPD) may be very deep or shallow depending on the heat flow in the region and composition of the rocks. The shallow CPD region is preferred as compared to the deep depth due to the cost of exploitation. A Curie temperature of 580 °C for magnetite is considered applicable to continental crust because magnetite is the most common magnetic mineral (Tanaka *et al.*, 1999). The Gamma rays arising from the decaying of unstable nuclei in the earth's rocks are recorded in this survey. The major elements that are of interest in the radiometric investigation are uranium, <sup>238</sup>U, thorium, <sup>232</sup>Th and potassium, <sup>40</sup>K (Keary *et al.*, 2002). Though, contributions from radio-elements in the subsurface to geothermal heat production would assist in the assessment of potential zones for geothermal resources and its possible exploitation. Nevertheless, to determine the CPD within a particular region of interest around the world several studies have been conducted: California, U.S.A. (Ross *et al.*, 2006); Yellow stone National Park, U.S.A. (Bhattacharyya and Leu, 1975); Cerro Prieto geothermal area, Baja California, Mexico (Espinoso-Cardena and Campos-Enriquez, 2008); East and

South east Asia (Tanaka *et al.*, 1999); Kyushu Island, Japan (Okubo *et al.*, 1985); north east Japan (Okubo and Matsunaga, 1994); India (Rajaram *et al.*, 2009); south-central Europe (Chiozzi *et al.*, 2005); the African-Eurasian convergence zone in south-western Turkey (Dolmaz *et al.*, 2005); and Bulgaria (Trifonova *et al.*, 2009). However, several studies have been conducted to investigate the Curie point depths within Nigeria which include (Ezekiel, 2019; Nwankwo and Shehu, 2015; Kasidi and Nur., 2012; Bensen *et al.*, 2019; Abdulwahab *et al.*, 2019; Ayuba and Lawal 2019; Ibe and Uche 2020; but, to the best of my knowledge, no previous work in the area that assess the variation of Curie temperature with depth.

In this study, the CPD, geothermal gradient, heat flow, radiogenic heat generation and temperature to depth variation could be determine to assess the geothermal resource potential in the study area using high-resolution aeromagnetic and radiometric data.

### Location of the Study Area

The area of study covers Kano State and parts of Jigawa State. The area is bounded by latitude 11° ' – 13° N and longitude 8° ' – 10° E (see figure 1a). The climate of Kano state is the tropical wet and dry type which is marked by two distinctive conditions: the rainy season which usually lasts from June to September, and the dry season which is hot with temperatures exceeding 39°C. February, March, and April are the hottest months, with day time temperatures exceeded to 45°C (Balogun, 2003). The natural vegetation of the study area is that of the Sudan Savannah type. The area of study lies on the Basement Complex of northern Nigeria (Figure 1b). The Nigerian basement complex is made up of gneisses, migmatites, and metasediments of Proterozoic

age which was intruded by series of granitic rocks of later Precambrian to Lower Palaeozoic age. These rocks were variably metamorphosed and granitized through the tectonic-metamorphic cycles converted to migmatites and granite-

gneiss (McCurry, 1971). Younger Granites rocks series were also noticed to be present within the area (Falconer *et al.*, 1911) and these are of the Jurassic in age, as well as volcanic, and occasional younger dikes.

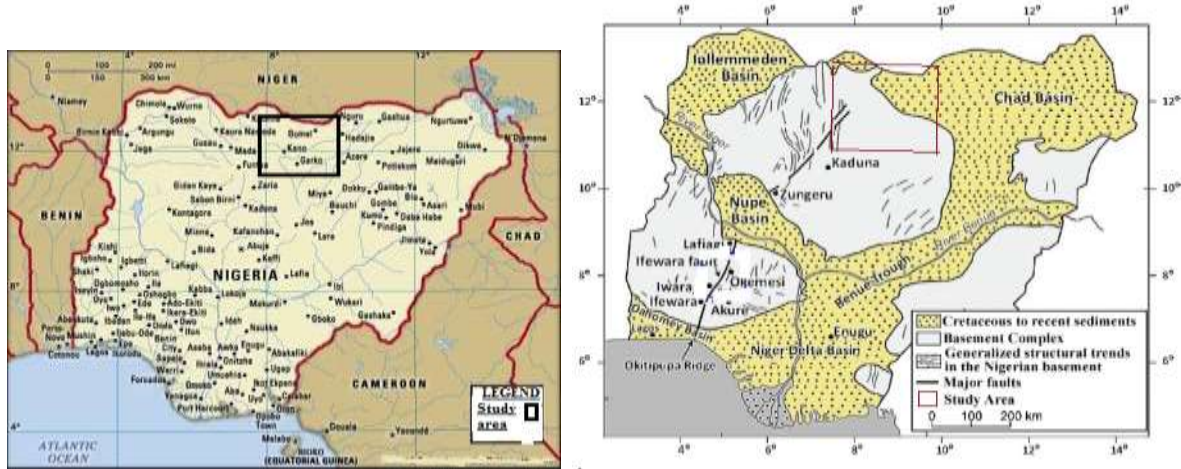


Figure 1: Map of Nigeria showing (a) the location of the study area (After, Britannica, 1914), (b) Geology of the study area (after NGSA, 2004)

**Data Acquisition and Processing**

The high-resolution aeromagnetic (HRAM) data was acquired by Fugro Airborne Survey from 2003 to 2010 using seven Cessna Caravan fixed-wing aircraft each carrying three Scintrex Cesium vapor magnetometers. The survey was done on row spacing of 500 m with average topographic gap of 80 m, resulting in a total of about 2 million row-km of data. The data logging interval is 0.1 seconds or less than 7 minutes. The projection methods used to process the data are Universal Transverse Mercator (UTM) and WGS 84 as a reference. The ellipsoid model of Clarke 1880 (modified), 33°E central meridian, zoom factor of 0.9996, 500,000 m X-deviation, 0 m Y-deviation were adopted. Also, 50 m grid size for drawing specifications and IGRF 2005 model were used for magnetic

declination and inclination calculations. The sixteen (16) Sheets of HRAM data of the study area were windowed to the dimension of 55x55 km. The Fugro stored the acquired data in the following format; Column X represents longitude/easting, column Y represents latitude/northing, and column Z represents total magnetic field intensity. Thus, for ease of handling of the data, the total magnetic field strength value (Z) of 33,000 nT was removed. Therefore, after obtaining the data from NGSA to derive Z total (TMI), these values must be compensated in each value for column Z. The X and Y columns were geo-referenced in the UTM projection system and then set as the preferred columns. Thereafter, the data were gridded to generate total magnetic field intensity (TMI) of the study area.

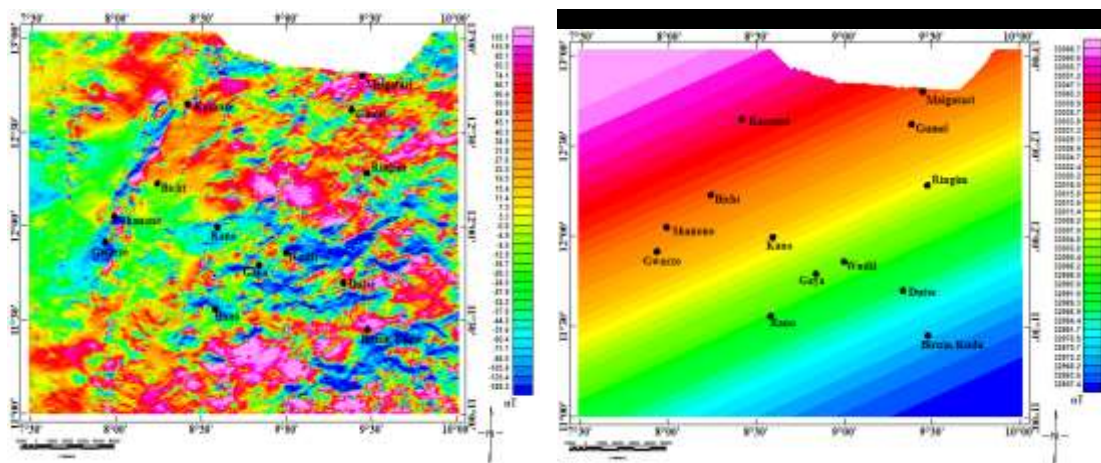


Figure 2: (a) Residual field map of the study area, (b) Regional field map of the study area.

Each of the 16 blocks of the gridded aeromagnetic data were subjected to various data processing techniques such as regional-residual separation (figure 2a & b), zero-padding, tapering, and fast-Fourier transform. Thereafter, the spectral centroid analysis method was applied to estimate the Curie point depths in the study area using the Step-by-step filtering option on the MAGMAP menu of Oasis Montaj.

**METHODOLOGY**

The estimation of Curie point depths of each blocks was done by using the Spectral analysis of the processed magnetic data and hence the assessment of the geothermal resources potential of the study area. There exist different approaches for carrying out estimation of depth to the bottom of magnetic sources. More so, the centroid method is one of the most commonly used approaches because it gives better estimates to depths with fewer errors compared with others (Ravat *et al.*, 2007).

**Table 1: Thermal Conductivity and Density of Common Rocks within the Study Area (From Cermak&Rybach, 1982, Horai, 1971 and Schon, 1996)**

S/N	ROCK TYPE	THERMAL CONDUCTIVITY RANGES (W/m°C)	DENSITY RANGES	MEAN THERMAL CONDUCTIVITY (W/m°C)	MEAN DENSITY g/cm <sup>3</sup>
1.	Alluvium	1.38 – 2.70	0.90 – 1.50	2.04	1.2
2.	Dolorite	2.02 – 2.62	2.54 – 3.38	2.32	2.95
3.	Shale	1.05 – 1.45	2.08 – 2.78	1.25	2.43
4.	Limestone	2.50 – 3.23	2.20 – 3.14	2.85	2.7
5.	Granite	1.9 – 3.2	2.55 – 2.74	2.55	2.65
6.	Clay	1.38 - 2.70	0.90 – 1.50	2.04	1.2
7.	Migmatite	2.39 – 3.41	2.43 – 287	2.9	2.65
8.	Schist	0.25 – 2.8	2.64 – 2.88	1.53	2.76
9.	Gneiss	0.94 – 4.86	2.57 – 2.88	2.9	2.65
10.	Silicate	2.41-3.39	1.98 – 3.32	2.9	2.65
11.	Sandstone	2.5 – 3.2	2.0 – 2.6	2.85	2.85
12.	Quartz	0.89 – 2.03	2.34 -2.96	1.46	2.65

The mathematical models of the centroid method are based on the assessment of the shape of isolated magnetic anomalies in crust introduced by Bhattacharyya and Leu (1975; 1977) and the study of the statistical properties of magnetic ensembles by Spector and Grant (1970). Consequently, the introduction of power spectral density of total magnetic field by Blakely (1995), Tanaka et al. (1999) reveals that the depths to the top bound and centroid of magnetic sources could be calculated from the power spectrum of magnetic anomalies. Hence, the basal (bottom) depth of the magnetic sources will be obtained from it.

The centroid depth is obtained from the low wave number part of the wave number-scaled power spectrum using the relation as shown in equation 1:

$$\ln(p(k) 1/2 / k = A - |k|Z_o \tag{1}$$

Where,  $p(k)$  is power spectrum,  $k$  is wave number,  $A$  is a constant and  $Z_o$  is the centroid depth.

Similarly, the depth to the top of the magnetic sources is derived from the slope of the medium to high wave number portion of the power spectrum using the relation in equation 2:

$$\ln(p(k) 1/2 = B - |k|Z_t \tag{2}$$

Where,  $B$  is a constant and  $Z_t$  is depth to the top of magnetic sources. Fitting the slope to a higher wave number part of the spectrum as suggested by Tanaka et al. (1999) leads to deeper magnetic bottom estimation that, at times, appear to be desirable (Ravat et al, 2007).

The depth to the bottom of the magnetic source ( $Z_b$ ) which is considered as the CPD is obtained from the relation in equation 3, as (Okubo et al., 1985):

$$Z_b = 2Z_o - Z_t \tag{3}$$

The geothermal parameters were obtained using the basal depth ( $Z_b$ ) information; the geothermal gradient ( $dT/dZ$ ) can be estimated from the relation shown in equation 4 (Tanaka et al, 1999; Ross et al, 2006):

$$dT/dZ = \theta_c / Z_b \tag{4}$$

Where,  $\theta_c$  is the Curie-temperature. The Curie-temperature depends on magnetic materials in the rock, but magnetite ( $Fe_3O_4$ ) is the most common magnetic mineral in igneous rock and has an approximate Curie-temperature of 580°C.

The heat flow ( $q_z$ ) of the study area was estimated using equation 5:

$$q_z = -k(dT/dZ) \tag{5}$$

Where  $k$  is thermal conductivity (Table 2) and  $(dT/dz)$  is the geothermal gradient, as Tanaka et al., (1999). According to Braun, (2009), the conductivity of the rock decreases as temperature increases, this means that the thermal conductivity in the lower crust is much lower than in the surface. The relationship between the thermal conductivity and the temperature changes was studied by Robertson, (1988).

The negative sign indicates the direction of the heat flow which moves in the opposite direction to the depth. This result was also compared with the heat flow of the geothermal fields in the region and these defined zones with geothermal resource potential in the area of interest.

**Interpretation of Radiometric Data**

The radio-elements are mostly the elements of radioactive origin which include, Uranium (U), Thorium (Th) or Potassium (K). The contributions of these elements are found in abundance in rocks of earth’s crust. This study is only concern with U, Th and K which are discussed as follow:

In this study, a total of four (4) sheets of airborne radiometric dataset of the anomalous CPD zone (hotspot) within the study area were obtained from the Nigerian Geological Survey Agency.

The radiometric data was gridded to obtain the values of each radioelement in all the blocks within the study area and these values were used to determine the radiogenic heat generation, concentration of radio-elements and temperature to depth variation model maps in the study area. The purpose of gridding the data is to identify and interpret signatures related with the source rocks for potential geothermal sources within the area under study.

**Determination of Radioactive Heat Production**

The three most pronounce types of isotope decay series abundant in rocks are the uranium series (decay of <sup>238</sup>U and <sup>235</sup>U), the thorium series (decay of <sup>232</sup>Th), and the decay of the potassium isotope <sup>40</sup>K. The radioactive heat production (Hp) as a result of isotope decay is expressed after Rybach (1976) as shown in equation 6:

$$Hp = 9.25Cu + 2.56Cth + 3.48Ck \tag{6}$$

Where, Hp is the radioactive heat production and C is concentration of each of the three mentioned radio-elements.

**Determination of Radiogenic Heat Generation**

The radiogenic heat generation (Rhg) in  $\mu W/m^3$  produced by rock radioactivity with concentrations of uranium (Cu), thorium (C<sub>Th</sub>) and potassium (C<sub>K</sub>) was estimated using the values of radioactive heat production and the density of the

rock types (Table 1) as shown in equation 7 as (Rybach, 1988).

$$R_{hg} = 10^{-5} \rho H_p \tag{7}$$

Where  $H_p$  is radioactive heat production,  $\rho$  is density of the rock (in  $kg/m^3$ ) (Table 1), U and Th are concentration of uranium and thorium (in ppm), while K is the concentration of potassium (in %). The computed values of radiogenic heat generation of the within the study area were used to produce the map of radiogenic heat generation in the area.

**Temperature to Depth Variation Model**

The temperature to depth variation model was estimated using equation 8 which was obtained from the linear relation and exponential distribution from Ravat et al., 2016. The relation was drive by obtaining a solution of the 1- Dimensional heat flow

equation. Thus, this relation was used to determine the temperature to depth variation within the study area.

Therefore, the values of the temperature to depth variation within the study area were obtained using model (equation 8) by varying the depths (Z) from 0 km, 2 km, 4 km, 6 km, 8 km and 10 km in the study area.

$$\theta_z = \theta_s + \frac{q_s Z}{K} + \frac{A_s b(b-Z)}{K} - \frac{A_s b^2 \exp(-Z/b)}{K} \tag{8}$$

where;  $q_s$  is heat flow obtained from the magnetic data;  $A_s$  radiogenic heat generation;  $\theta_z$  is temperature at Z-depth (temp-to-depth variation);  $\theta_s$  surface temperature (from Schoenech and Askira 1987); b is the empirical heat production depth distribution parameter (assumed to be 10 km) as (Ravat et al., 2016) and k is thermal conductivity of the rock types (Table 1).

**RESULTS**

**Results from Magnetic Data**

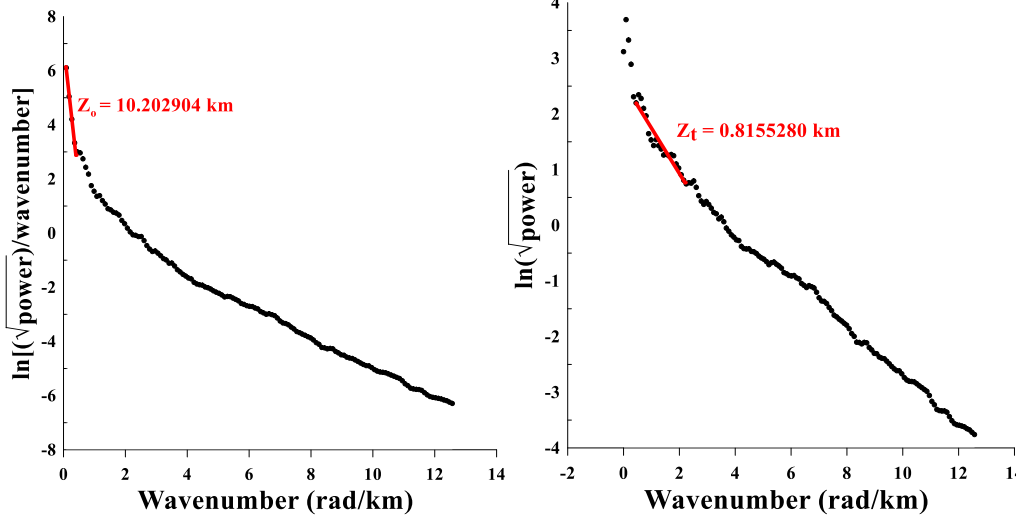


Figure 3: Spectral plot for block 35 of the study area.

Table 2 presents the results of the estimated depths for the 16 blocks of the gridded aeromagnetic data of the study area. The depths to the top of magnetic sources range from 0.82 km to 1.24 km with an average of 1.03 km. Also, the depths to the centroid of the magnetic sources in the study area range from 2.66 km to 10.20 km with an average of 6.43 km. The values were used in calculating the CPD (equation 3) of the study area, which range from 4.27 km to 19.59 km with an average of 11.83 km.

From CPD map (figure 4) shows areas of Shallow and Deep Curie point depth. The shallow zones have values ranging from 4.27 km to 11.07 km (hotspot) covering the central part, NE, northern and southern boundaries, including places like Kano, Bichi, Ringim, Gaya, Wudil, Rano, Maigatari and Gumel. The deep Curie point depth zones have values ranging from 11.38 km to 19.59 km, observed in the north, NW; SW and SE boundaries including places like Birnin Kudu, Dutse, Shanono, Gwarzo and Kazaure.

**Table 2: showing computed result of the spectral analyses of the study area.**

S/N	BLOCK No	Z <sub>t</sub> (km)	Z <sub>o</sub> (km)	CPD (km)	Geothermal gradient (°C/km)	Heat Flow (mW/m <sup>2</sup> )	Longitude	Latitude	Rocks Types
1.	35.	0.816	10.203	19.590	29.606	74.016	8.25	12.75	Migmatite
2.	36.	0.926	5.880	10.834	53.538	133.844	8.75	12.75	Granite
3.	37.	0.825	6.503	12.181	47.614	119.035	9.25	12.65	Alluvium
4.	38.	0.921	5.114	9.307	62.322	155.804	9.75	12.75	Alluvium
5.	57.	1.039	2.657	4.274	135.695	339.237	8.25	12.25	Granite
6.	58.	1.111	5.187	9.262	62.622	156.554	8.75	12.25	Granite
7.	59.	0.937	5.368	9.800	59.183	147.959	9.25	12.25	Alluvium
8.	60.	1.233	5.120	9.007	64.393	160.982	9.75	12.25	Alluvium
9.	80.	1.001	5.661	10.321	56.199	140.497	8.25	11.75	Migmatite
10.	81.	0.988	5.123	9.257	62.654	156.635	8.75	11.75	Granite
11.	82.	1.059	6.443	11.827	49.039	122.597	9.25	11.75	Granite
12.	83.	1.236	5.568	9.900	58.584	146.461	9.75	11.75	Alluvium

13.	103.	1.011	6.484	11.957	48.507	121.267	8.25	11.25	Granite
14.	104.	0.877	5.855	10.833	53.542	133.855	8.75	11.25	Granite
15.	105.	0.992	8.747	16.503	35.145	87.864	9.25	11.25	Granite
16.	106.	0.968	6.259	11.550	50.219	125.546	9.75	11.25	Granite

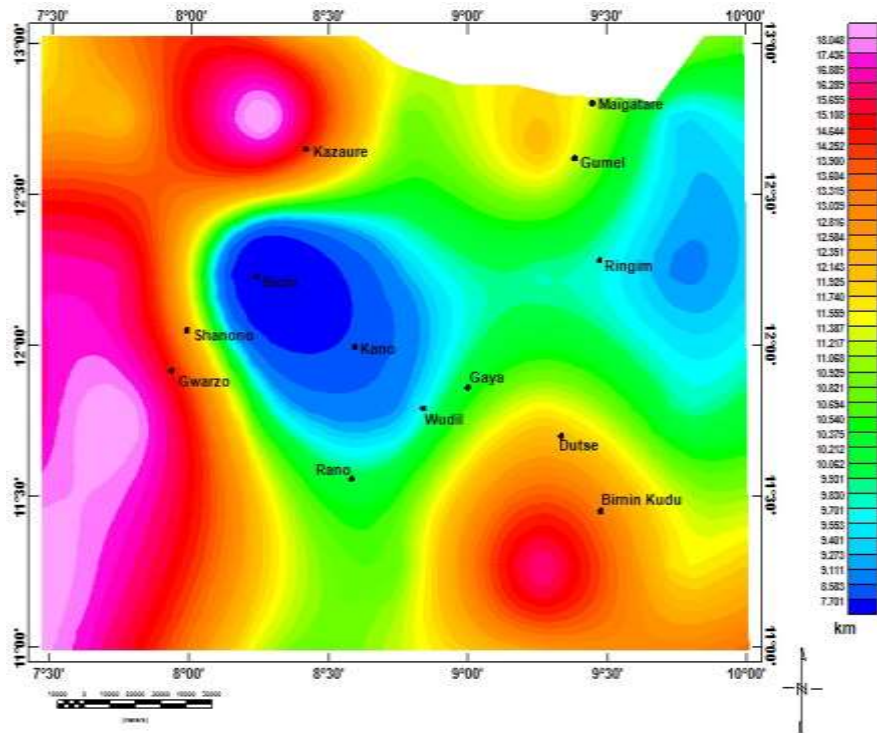


Figure 4: Map of CPD of the study area

The map of the geothermal gradient (figure 5) of the study area was obtained using equation 4. The calculated values (Table 2) were used to produce the geothermal gradient map of the study area. The result shows that the values range from 35.2 °C/km to 135.7 °C/km with average value of 85.5 °C/km. Also, from the map shows two distinct locations of temperature changes with depth. The location observed with

high geothermal gradient ranging from 62.3 °C/km to 135.7 °C/km covers the central parts of the study area, in places like Kano, Bichi, Shanono, Wudil, Kazaure, Ringim and through the Eastern boundary. Low geothermal gradient was observed at the Northern, Western and the Southern boundary of the study area.

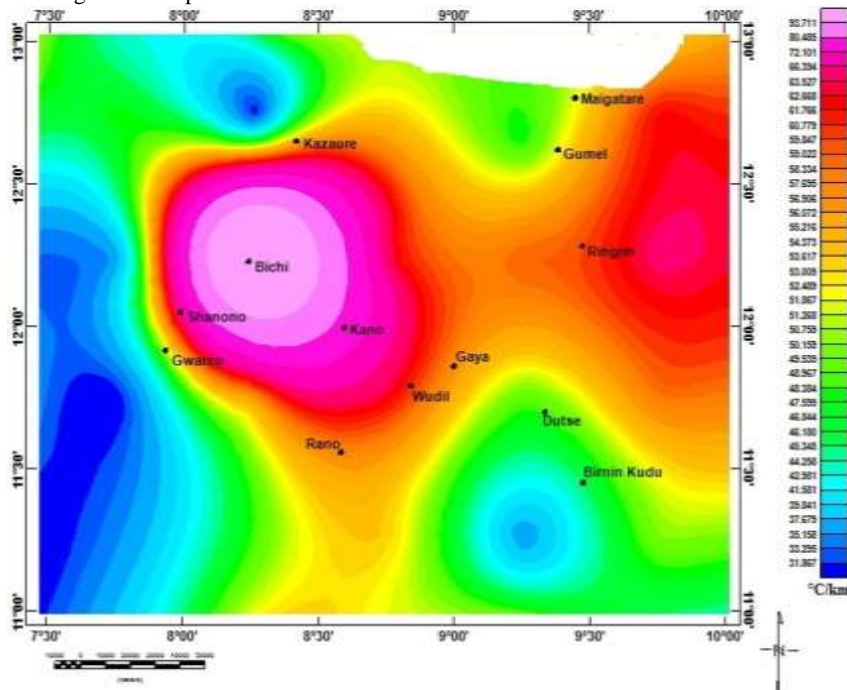


Figure 5: Map of geothermal gradient of the study area.

The heat flow values of the area were obtained using equation 5, the computed values of the geothermal gradient (Table 2) and thermal conductivity (Table 1) of each rock type within the study area. The values were used to produce the heat flow map (figure 6) of the study area. The heat flow values of the area range from 74 mW/m<sup>2</sup> to 339.2 mW/m<sup>2</sup> with the average of 206.6 mW/m<sup>2</sup>. From the heat flow map, it is observed that the study area is divided into areas low and high heat flow.

The values of the Low heat flow areas range from 74 mW/m<sup>2</sup> to 87.9 mW/m<sup>2</sup>, are observed in the Northern parts, including Maigatari, Gumel and Birnin Kudu, the western and southern boundaries. These locations correspond to areas of deep Curie point depth and low geothermal gradient. Furthermore, high heat flow values in the area range from 119 mW/m<sup>2</sup> to 339.2 mW/m<sup>2</sup>, and was observed in the central part, through the NE, NW and southern boundaries including places like Kano, Bichi Shanono, Wudil, Rano, Gwarzo, Gaya and Kazaure.

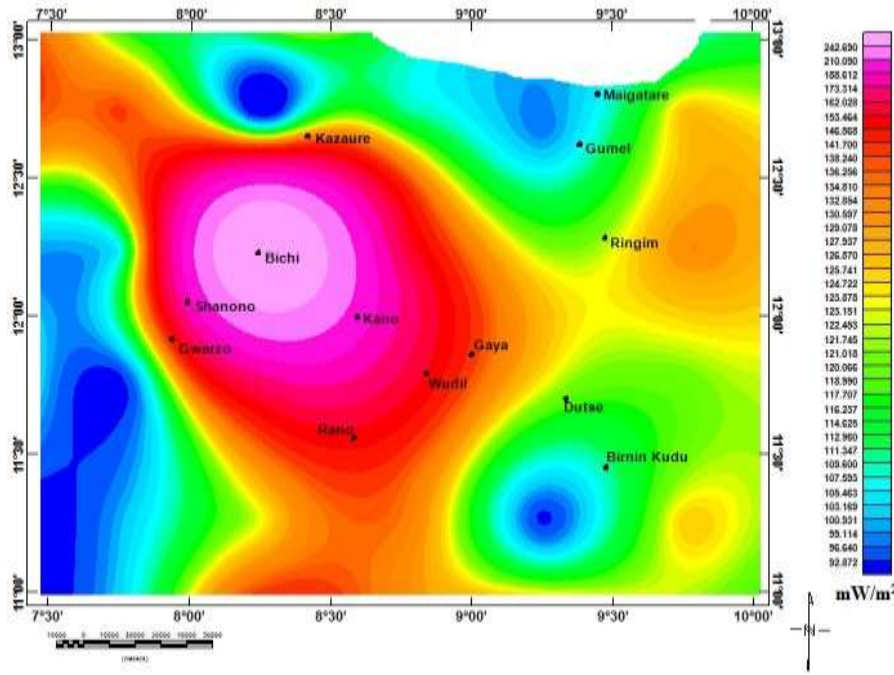


Figure 6: Map of Heat flow of the study area

**Results from Radiometric Data**

In addition to the heat coming from the upper mantle, one parameter needed, to estimate the geothermal resource, is radiogenic heat generation which is produced by decay of radioactive elements, majorly U, Th, and/or K, in the crust which is an important contributor to heat flow at the surface (Clauser, 2011). Therefore, in order to obtain a clear picture of the result from this investigation, the study also adopts the radiometric method to determine the radiogenic heat generation of the CPD anomalous region within the study area. Radiometric data of the shallow CPD region which was considered as a geothermal hotspot in the area was obtained and used to investigate the radiogenic heat generation and temperature to depth variation of the study area. Aside heat source due to earth’s crust (CPD), radioactivity is another

source of heat contributor that established a geothermal resource potential in the continental crust.

The result (figure 7) shows high concentration of potassium (K) at the central and southern boundary with values ranging from 0.87 % to 2.93 % , low K concentration dominates the northern boundary with values ranging from 0.12 % to 0.84 % . More so, figure 8 reveals high concentration of Thorium (Th) at the SW and southern boundary of the area with values ranging from 12.08 ppm to 22.02 ppm, low Th concentration was observed in the NE boundary with values from 3.81 ppm to 11.82 ppm. Also, figure 9 shows high concentration of Uranium (U) at the SW, central part through the southern boundary with values ranging from 2.01 ppm to 5.39 ppm, low U concentration was observed in the NE boundary with values ranging from 0.12 ppm to 1.94 ppm.

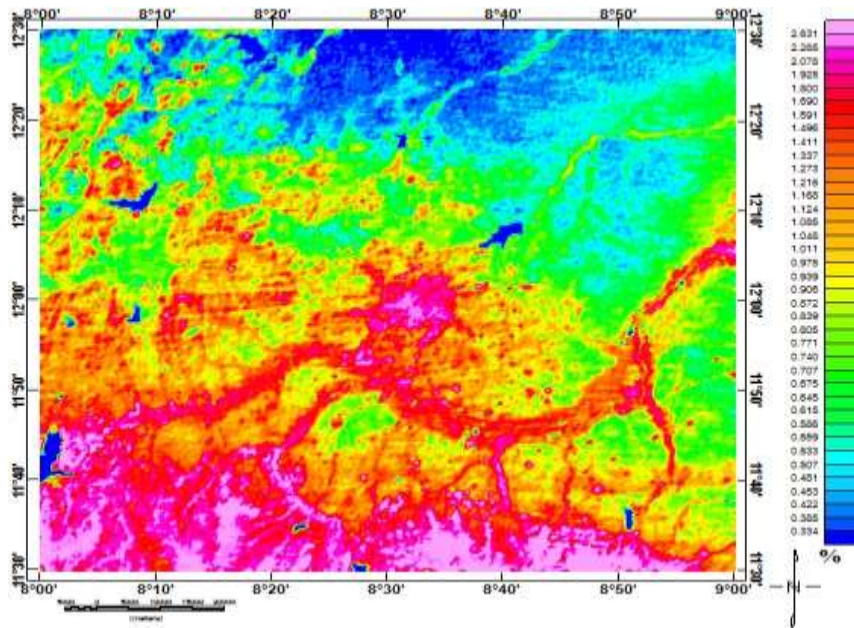


Figure 7: Map of Potassium concentration within the study area.

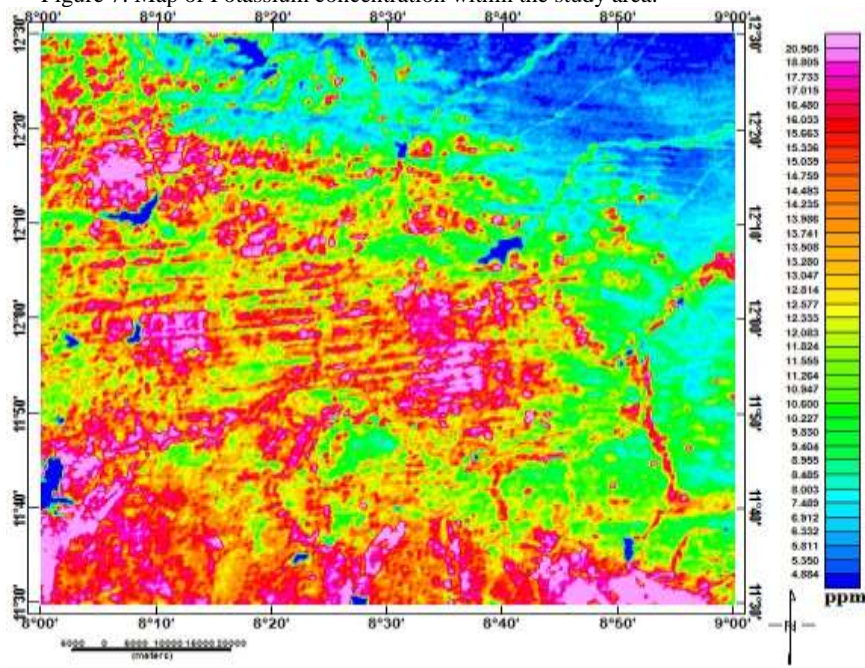


Figure 8: Map of Thorium concentration within the study area.

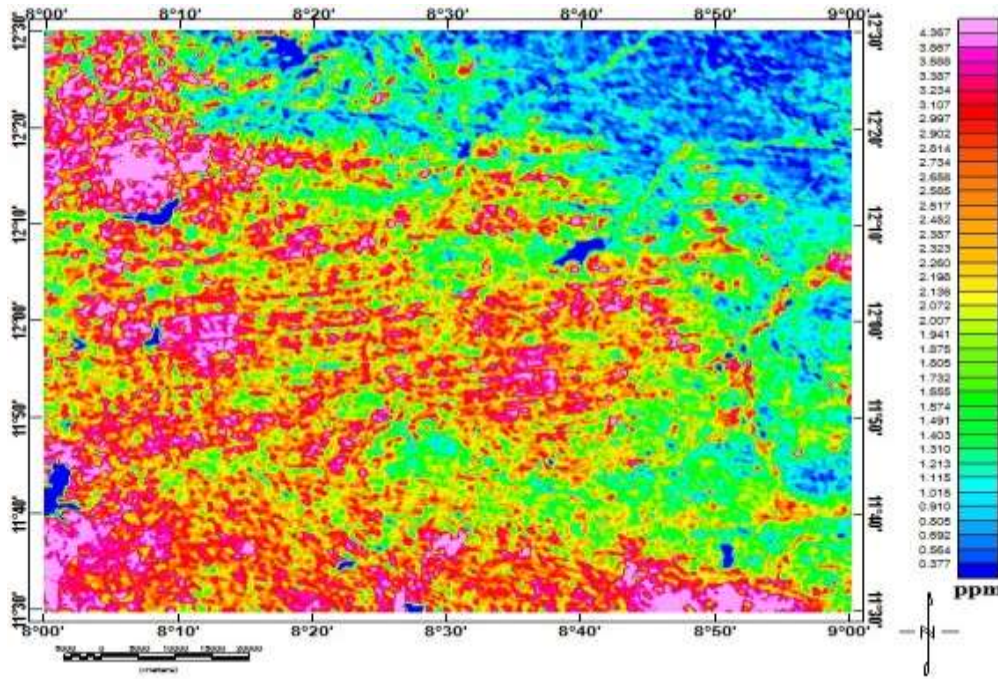


Figure 9: map of Uranium concentration within the study area.

**Distribution of U, Th & K within the Study Area**

The compositions of K, Th and U were shown in the Ternary map of the study area. Ternary presented triangular plots of the radio-elements (figure 10) which displayed images by combining the three radio-elements which are also useful in

classifying some rock types within the study area. Moreover, ternary plots of the radio-elements usually give a superior image of the geology (Salem et al., 2005).

Figure 10 show that Uranium occupied almost the entire central part through the NW boundary of the study.

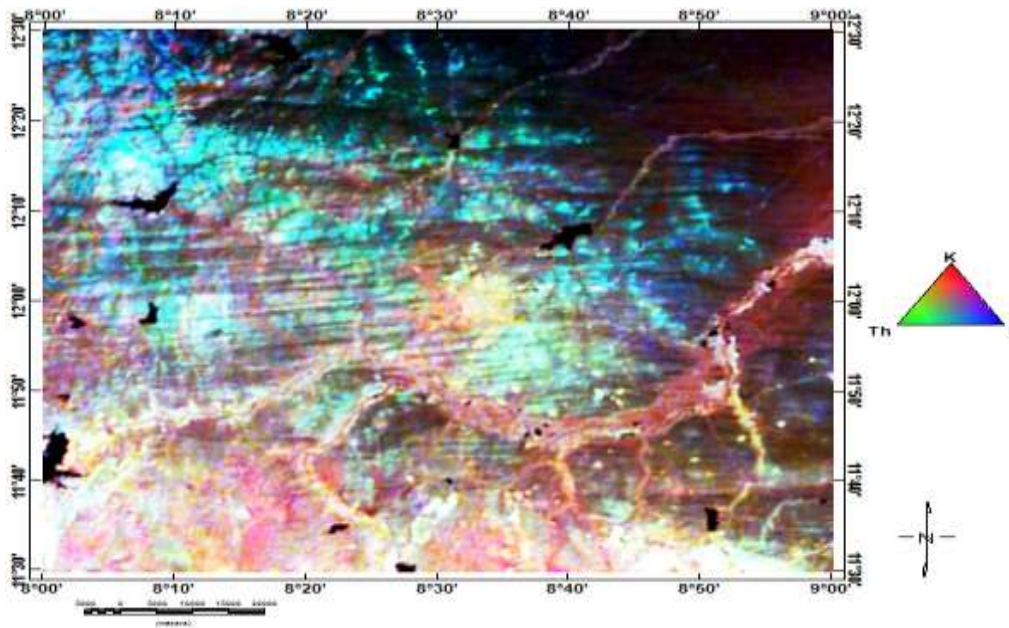


Figure 10: Ternary Map of K, Th & U within the study area.

**Radiogenic Heat Generation**

The radiogenic heat (Rhg) generation (figure 11) produced by rock radioactivity with concentrations of uranium ( $C_U$ ), thorium ( $C_{Th}$ ) and potassium ( $C_K$ ) was determined by using equation 7.

Figure 11 shows high values of radiogenic heat generation ranging from  $1.33 \mu W/m^3$  to  $2.77 \mu W/m^3$  was observed in the

NW, SW through the central parts and to the southern boundary. Low radiogenic heat generation values ranging from  $1.29 \mu W/m^3$  to  $0.32 \mu W/m^3$  was observed in the entire north and NE boundaries of the study area, including places like Bichi, Kano and Wudil.

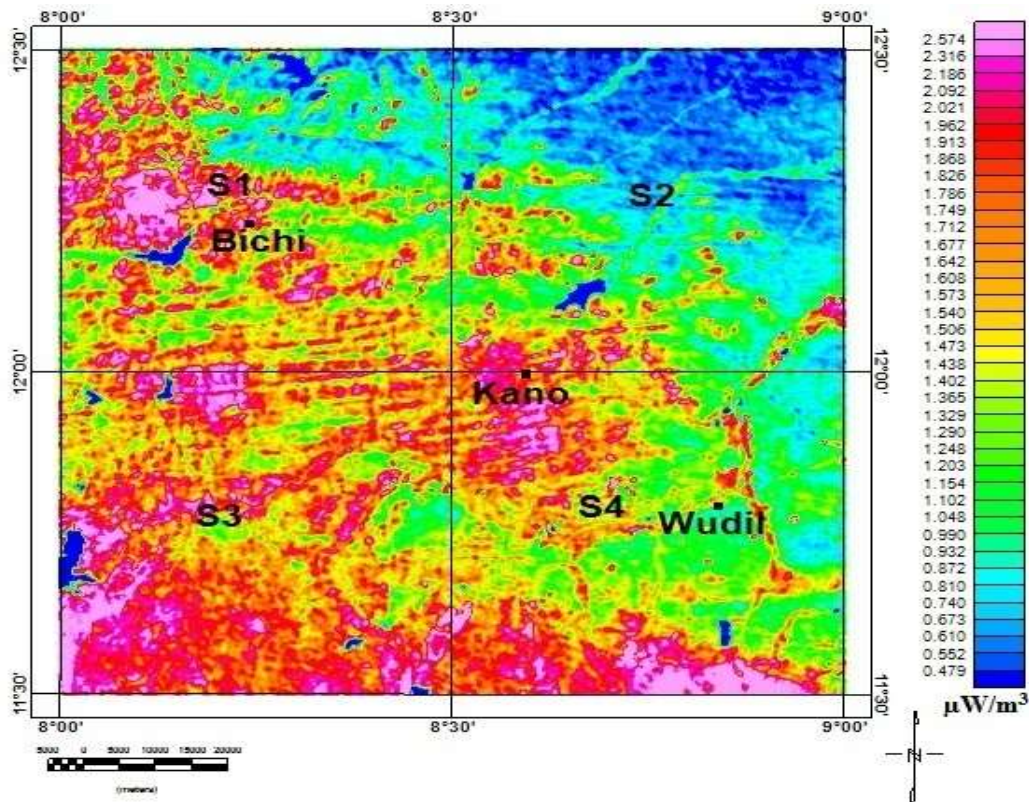


Figure 11: Radiogenic heat generation map of the study area.

**Temperature to Depth Variation Model**

The model presents how temperature changes from the surface to a given depth in the crust. It also provides information about the temperature range at a particular depth, thus reveals the depth at which Curie temperature could be attained.

Table 3 shows the estimated values of temperature to depth variations of the hotspots in the study area. The values were determined using the solution of a 1 - dimensional heat equation as shown in equation 8.

**Table 3: Computed values of temperature to depth variation within the study area**

DEPTHS	0 km	2 km	4 km	6 km	8 km	10 km
	26	295.975	563.468	828.930	1092.728	1355.163
TEMPERATURES	26	150.120	272.271	392.810	512.029	630.167
(°C)	26	137.063	245.787	352.595	457.835	561.790
	26	149.494	269.806	387.513	503.087	616.914

The temperature to depths variation values in tables 3 were used to plot the temperature against depth graph which is the pictorial representation of the model. The result shows that at depth of 6 km 8 km and 10 km. The plot reveals that some points have temperature values greater than the Curie

temperature as assumed for magnetite rocks (> 580 °C). Thus, at depths of 2 km and 4 km the temperature was shown to have values less than the Curie temperature (see figure 12).

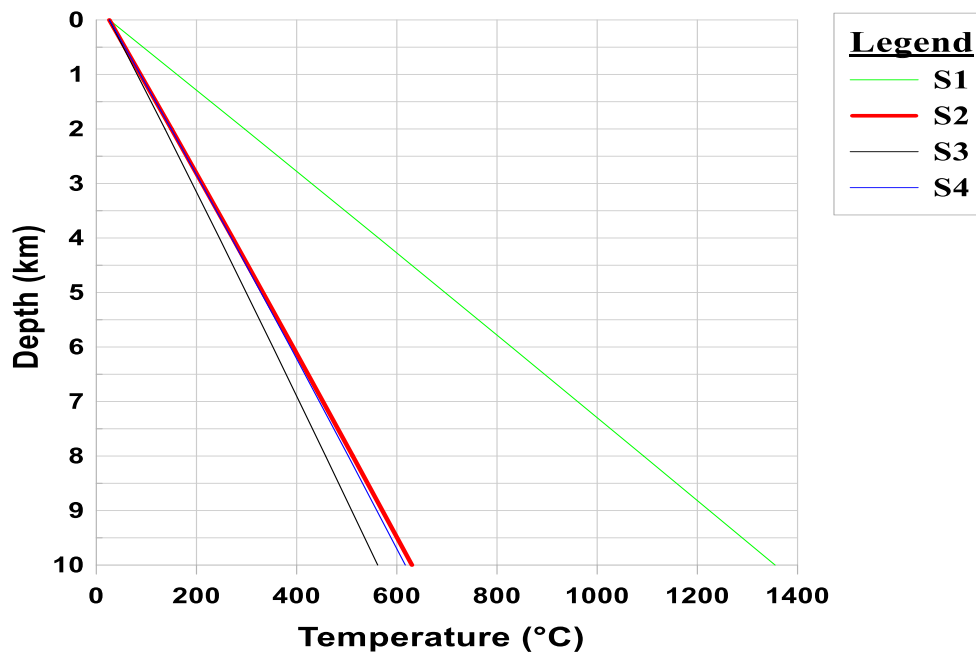


Figure 12: plot of Temperature to depth variation within the geothermal hotspot in the study area.

**DISCUSSIONS**

It was observed that Curie point depth in the study area varies from 4.27 km to 19.59 km with an average of 11.83 km. The shallow CPD zones have values ranging from 4.27 km to 11.07 km and is considered to be geothermal hotspots within the study area, covering the central part, NE, northern and southern boundaries, including places like Kano, Bichi, Ringim, Gaya, Wudil, Rano, Maigatari and Gumel. Similarly, the deep Curie point depth zones have values ranging from 11.38 km to 19.59 km was observed in the north, NW; SW and SE boundaries that include places like Birnin Kudu, Dutse, Shanono, Gwarzo and Kazaure. Shallow Curie isotherm depths are ascribed to where the crust is thin while deeper curie isotherm depths could be as a result of thick crust isostatic compensation in the region (Kasidi and Nur, 2012). In other words, shallow Curie point depth indicates Crustal thinning/Updoming/ Intrusion which also lead to high temperature in the affected area (Nwankwo and Shehu, 2017). Therefore, the shallow CPD regions suggest crustal thinning while regions with deep CPD imply the crust thickens. The shallowest CPD regions (hotspot) was identified, and selected for further analysis of radiogenic heat generation, and temperature-depth variation.

The values of geothermal gradient (rate of change in temperature with depth) of the study area range from 29.6 °C/km to 135.7 °C/m with an average of 82.7 °C/km. The region with low geothermal gradient was observed at the northern, western and the southern boundaries. Likewise, high geothermal gradient was shown to have values ranging from 62.3 °C/km to 135.7 °C/km at the central parts of the study area, including places like Kano, Bichi, Shanono, Wudil, Kazaure, Ringim and eastern boundary. It was observed that areas with deep Curie point depth correspond to low geothermal gradient and similarly, low Curie point depth zones match up with portions observed to have high geothermal gradient.

The heat flow ranges from 74 mW/m<sup>2</sup> to 339.2 mW/m<sup>2</sup> with the average of 206.6 mW/m<sup>2</sup>. The Low heat flow values ranges from 74 mW/m<sup>2</sup> to 87.9 mW/m<sup>2</sup>, are observed in the Northern parts, including Maigatari, Gumel and Birnin Kudu, the western and southern boundaries. Also high heat flow values in

the area range from 119 mW/m<sup>2</sup> to 339.2 mW/m<sup>2</sup>, and was observed in the central part, through the NE, NW and southern boundaries, including places like Kano, Bichi Shanono, Wudil, Rano, Gwarzo, Gaya and Kazaure. These places correspond to the areas of shallow Curie point depths and high geothermal gradient.

The average heat flow in a thermally normal continental crust is 60mW/m<sup>2</sup>, but average oceanic heat flow is 101 mW/m<sup>2</sup> (Jaupart and Mareschal, 2007). Heat flow values between 80 mW/m<sup>2</sup> to 100 mW/m<sup>2</sup> are an indication of viable good geothermal conditions (Ludvik, 2009). Meanwhile, a heat flow values greater than 100 mW/m<sup>2</sup> is suggests anomalous geothermal condition (Jessop et al., 1976). Therefore, it was shown that, almost the entire study area reveals high heat flow, >100 mW/m<sup>2</sup>, which suggest potential geothermal source of energy.

The average heat flow in a thermally normal continental crust is 60mW/m<sup>2</sup>, but average oceanic heat flow is 101 mW/m<sup>2</sup> (Jaupart and Mareschal, 2007). Heat flow values between 80 mW/m<sup>2</sup> to 100 mW/m<sup>2</sup> are an indication of viable good geothermal conditions (Ludvik, 2009). Meanwhile, a heat flow values greater than 100 mW/m<sup>2</sup> is suggests anomalous geothermal condition (Jessop et al., 1976). Therefore, majority of the study area have anomalously high heat flow, >100 mW/m<sup>2</sup>, which suggest potential geothermal source of energy.

The study area shows high values of radiogenic heat generation ranging from 1.33 μW/m<sup>3</sup> to 2.77 μW/m<sup>3</sup>, observed in NW, SW through the central part and southern boundary. Similarly, low values ranging from 1.29 μW/m<sup>3</sup> to 0.32 μW/m<sup>3</sup> was observed in the north and NE boundaries which include places like Bichi, Kano and Wudil.

This radiogenic heat value of 2.77 μW/m<sup>3</sup> is within the values reported for average continental crust radiogenic heat generation (Alistair et al., 2014; Wollenberg and Smith, 1987). The high concentration of uranium, potassium and thorium in the area also shows high potentiality for geothermal energy.

The ternary map shows that Uranium dominates almost the entire central part and the NW boundary of the study area and this indicates the presence of granites and pegmatites rocks in

the area. Potassium was observed in large amount at the SW and NE boundaries and indicates high concentration of felsic igneous basalt and granite rocks in the area. Thorium was observed in the area dominated by uranium and this reveals the presence of mafic igneous rocks in the area.

Thus, from the temperature to depth model in this study, it was found that, the Curie temperature could be attained at a minimum depth of 6 km within the area with shallow CPD regions. Therefore, based on the analysis from the CPD, geothermal gradient, heat flow, radiogenic heat and temperature to depth variation the study area could be considered geothermal energy potential region.

## CONCLUSION

The Curie point isotherm deduced from the study, indicate that the crust is thinning, shallow Curie point depth, in the Central and Eastern parts of the study area. The geothermal gradient shows that the area is classified into low and high temperature zones. High temperature zones could result into thermal maturation of sediments and hence probable oil generation. This study provides thermal information which could guide in geothermal energy exploitation within the study area. The areas with high heat flow were delineated and could be prospective for geothermal energy in generating electricity. The high concentration zones of Uranium and Thorium observed in the area is found to a trend extending to the western boundary which trend to Niger Republic across the mid-northern border. This concentration also follows the pattern of radiogenic heat generation in this area. The Curie temperature within the study area could be attained at the depth of 6 km, and sedimentary maturation could occur at a minimum depth of 2 km. Thus, the study area could be considered for geothermal resource exploitation in order to boost power (electricity) generation for domestic and industrial usage in the region.

## ACKNOWLEDGEMENT

The author is grateful to the Department of Physics Ahmadu Bello University Zaria for providing guide and facilities and also to Nigerian Geological Survey Agency (NGSA), for releasing the data used in carrying out this study.

## REFERENCES

Abdulwahab, M, Taiwo, A, Salako, A.K, Rafiu, A, Abbass A.A, and Alhassan, U. (2019). Assessment of Geothermal Potentials In Some Parts of Upper Benue Trough Northeast Nigeria Using Aeromagnetic Data; *Journal of Geoscience, Engineering, Environment, and Technology* Vol 04 No 01. doi: 10.25299/jgeet.4.1.2090.

Ayuba, M.G., and Lawal, M.K. (2019). Investigating Geothermal Energy Resource Potential in Parts of South Western Nigeria Using Aeromagnetic Data; *Science World Journal* Vol. 14(No 3).

Balogun, I. (2003). Rainfall and length of growing season in Nigeria International Research Institute for climate and society.

Bensen, I.E., Chinwuko, A.I., Ogah V.E., Akiishi, M., Usman, A.O., & Udoh, A.C. (2019). Curie-Temperature Depth and Heat Flow Deduced from Spectral Analysis of Aeromagnetic Data over the Southern Bida Basin, West-Central Nigeria; *Geosciences*, 9 (2): 50-56 doi: 10.5923/j.geo.20190902.02.

Bhattacharyya, B.K., and Leu, L.K. (1975). Analysis of magnetic anomalies over Yellowstone National Park: Mapping of Curie point isothermal surface for geothermal reconnaissance. *Journal of Geophysical Research*, 80 (32); 4461–4465, doi: 10.1029/JB080i032p04461.

Bhattacharyya, B.K., and Leu, L.K. (1977). Spectral Analysis of gravity and magnetic anomalies due to rectangular prismatic bodies. *Geophysics*, 42; 41–50 doi:10.1190/1.1440712.

Blakely, R.J. (1995). Potential theory in gravity and magnetic applications: Cambridge University Press.

Braun, J. (2009). Hot blanket in Earth's deep crust. *Nature*: 458(7236), 292–293. <https://doi.org/10.1038/458292a>.

Chiozzi, P., Matsushima, J., Okubo, Y., Pasquale, V., and Verdoya, M. (2005). Curie point depths from spectral analysis of magnetic data in central-southern Europe. *Physics of the Earth and Planetary Interiors*, 152(4); 267–276, doi:10.1016/j.pepi.2005.04.005.

Clauser, C., 2011, Radiogenic heat production of rocks, in Gupta, H., ed., *Encyclopedia of Solid Earth Geophysics*: Dordrecht, The Netherlands, Springer, p. 1018–1024, doi: 10.1007/978-90-481-8702-7\_74.

Dolmaz, M.N., Ustaomer, T., Hisarli, Z.M., and Orbay, N. (2005). Curie point depths variations to infer thermal structure of the crust at the African-Eurasian convergence zone, SW Turkey. *Earth, Planets and Space*, 57; 373–383.

Espinosa-Cardena, J.M., and Campos-Enriquez, J.O. (2008). Curie point depth from spectral analysis of aeromagnetic data from Cerro Prieto geothermal area, Baja California, Mexico. *Journal of Volcanology and Geothermal Research*, 176(4); 601–609, doi:10.1016/j.jvolgeores.2008.04.014.

Ezekiel, K. (2019). Geothermal Study Over Sokoto Basin Northwestern, Nigeria: *International Journal of Engineering Science Invention (IJESI) ISSN (Online): 2319 – 6734, ISSN (Print): 2319 – 6726*.

Falconer, J.D. (1911). The geology and geography of Northern Nigeria, MacMillan, London.

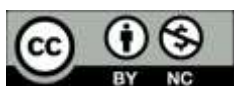
Ibe, S.O., and Uche, K.I. (2020). Assessment of Geothermal Energy Potential of Ruwan Zafi, Adamawa State and Environs, Northeastern Nigeria, using High Resolution Airborne Magnetic Data: Current Research in Geoscience 2020, Volume 10: 1.15; DOI: 10.3844/ajgsp.2020.1.15.

Jaupart, C, and Mareschal, J.C, (2007). Heat Flow and Thermal Structure of the Lithosphere; Institut de Physique du Globe de Paris, Paris, France, GEOTOP-UQAM-McGill, Montreal, QC, Canada.

Jessop, A.M., Habart, M.A., and Sclater, J.G. (1977). The world heat flow data collection 1975. Geothermal services of Canada Ser 50: 55.77.

Kasidi and Nur, A. (2012). Curie depth isotherm deduced from spectral analysis of Magnetic data over sarti and environs of North-Eastern Nigeria. *Scholarly Journals of Biotechnology* Vol. 1(3), Pp. 49-56. Nigerian Geological Survey Agency, NGSA. Geological Map of Latitude 11030' - 13030' and Longitude 4000' and 6000', 2006.

- Kearey, P., Klepeis, K.A., and Vine, F.J. (2009). Global tectonics, *John Wiley & Sons*.
- Lúdvík S. Georgsson (2009). Geophysical methods used in geothermal exploration United Nations University Geothermal Training Programme Orkustofnun, Reykjavik, ICELAND [lsg@os.is](mailto:lsg@os.is)
- Megwara, U.J., Udensi, E.E., Olasehinde, I.P., Daniyan, A.M., and Lawal K.M. (2013). Geothermal and Radioactive Heat Studies of Parts of Southern Bida Basin, Nigeria and the Surrounding Basement Rocks; *international journal of Basic and Applied Sciences* 2(1)123.
- Mccurry, P. (1989). A general review of the geology of the Precambrian to Lower Palaeozoic rocks of northern Nigeria. In: Kogbe, C. A. (ed) *Geology of Nigeria, 2 nd Ed.*, Rock View (Nigeria) Limited.
- Nigerian Geological Survey Agency (2004). Acquisition of Aeromagnetic and Radiometric data by Fugro airborne.
- Ofor, N.P., and Udensi, E.E. (2014). Determination of the Heat flow in the Sokoto Basin, Nigeria Using Spectral Analysis of Aeromagnetic Data. *Journal of Natural Science Research: Vol. 4, No. 6, Pp. 83-93*. <https://dx.doi.org/10.4314/ijns.v23i1.17>
- Nwankwo, L.I., and Shehu, A.T. (2015). Evaluation of Curiepoint depths, geothermal gradients and near-surface heat flow from high-resolution aeromagnetic (HRAM) data of the entire Sokoto Basin. *Journal of Volcanol Geothermal Research* Vol30 No5, pp 45–55.
- Nwankwo, L.I., and Sunday, A.J. (2017). Regional Estimation of Curie-point Depths and Succeeding geothermal parameters from recently acquired high-resolution aeromagnetic data of the entire Bida Basin, north-central Nigeria. *Geothermal Energy Science*, 5(1), 1.
- Okubo, Y., Graf, R.J., Hansen, R.O., Ogawa, K., and Tsu, H. (1985). Curie point depths of the island of Kyushu and surrounding area, Japan; *Geophysics*, 50 (3) 481–489, doi: 10.1190/1.1441926.
- Okubo, Y., and Matsunaga, T. (1994). Curie point depth in northeast Japan and its correlation with regional thermal structure and seismicity. *Journal of Geophysical Research*, 99 (B11); 22363–22371, doi:10.1029/94JB01336.
- Rajaram, M., Anand, S.P., Hemant, K. and Purucker, M.E. (2009). Curie isotherm map of Indian subcontinent from satellite and aeromagnetic data. *Earth and Planetary Science Letters*, 281(3–4); 147–158, doi:10.1016/j.epsl.2009.02.013.
- Ravat, D., Pignatelli, A., Nicolosi, I., and Chiappini, M. (2007). A study of spectral methods of estimating the depth to the bottom of magnetic sources from near-surface magnetic anomaly data, *Geophysical Journal International*, 169: 421–434.
- Ravat, D, Morgan, P. and Lowry, A.R., (2016). Geotherms from the temperature-depth-constrained solutions of 1-D steady-state heat-flow equation *Geosphere*, V. 12, no. 4, p. 1187–1197, doi:10.1130/GES01235.1.
- Robertson, E.C. (1988). Thermal properties of rocks. Report 88-441. *US Department of the Interior: Geological Survey*, 106. <https://doi.org/10.3133/ofr88441>.
- Ross, H.E., Blakely, R.J., and Zoback, M.D. (2006). Testing the use of aeromagnetic data for the determination of Curie depth in California. *Geophysics*, 71(5) L51–L59, doi: 10.1190/1.2335572.
- Rybach, K., Hokrick, R., and Eugester, W. (1988). Vertical earth probe measurements and prospects in Switzerland, *Commun. Proc.* 1 67–372.
- Salem, A., Abouelhoda, E., Alaa, A., Atef, I., Sachio, E., and Keisuke, U. (2005). Mapping Radioactive Heat Production from Airborne Spectral Gamma-Ray Data of Gebel Duwi Area, Egypt. *Proceedings World Geothermal Congress, Antalya, turkey*, 24-29.
- Schoenech and Askira (1987). Map of surface temperature ranges within Nigeria.
- Spector, A., and Grant, F.S. (1970). Statistical model for interpreting aeromagnetic data. *Geophysics*, 35(2); 293–302.
- Tanaka, A., Okubo, Y., and Matsubayashi, O. (1999). Curie point depth based on spectrum analysis of the magnetic anomaly data in East and Southeast Asia. *Tectonophysics*, 306(3–4); 461–470.
- Trifonova, P., Zhelev, Z., Petrova, T., and Bojadgieva, K. (2009). Curie point depths of Bulgarian territory inferred from geomagnetic observations and its correlation with regional thermal structure and seismicity. *Tectonophysics*, 473(3–4); 362–374, doi:10.1016/j.tecto.2009.03.014.
- Wollenberg, H.A., and Smith, A.R., (1987). Radiogenic heat production of crustal rocks: An assessment based on geochemical data: *Geophysical Research Letters*, v. 14, p. 295–298, doi: 10.1029/GL014i003p00295.



©2022 This is an Open Access article distributed under the terms of the Creative Commons Attribution 4.0 International license viewed via <https://creativecommons.org/licenses/by/4.0/> which permits unrestricted use, distribution, and reproduction in any medium, provided the original work is cited appropriately.